

## Structural Analysis of High-Resolution Aeromagnetic Data over Naraguta Area, Nigeria: Implications for Hydrothermal Mineralization Potentials

*Stella C. Okenu<sup>1</sup>, Oluseyi G. Oyerinde<sup>1</sup>, Ayuba J. Bwamba<sup>1</sup>, Jumoke O. Fatoba<sup>1</sup>, Eze M. Okoro<sup>2\*</sup>*

<sup>1</sup> *Sheda Science and Technology Complex, Abuja, Nigeria*

<sup>2</sup> *Department of Geology, University of Nigeria Nsukka, Enugu State, Nigeria*

Received March 26, 2024; Accepted July 10, 2024

---

### Abstract

High-resolution aeromagnetic (HRAM) data covering the Naraguta area was analyzed to map structural features that may influence the formation of hydrothermal mineral alteration in the area. The aeromagnetic data was filtered by applying enhancement algorithms like first vertical derivative (1VD), analytical signal (AS) and horizontal gradient magnitude (HGM) to delineate the boundaries of linear geological structures and identify potential mineralization zones. Spectral analysis method was used to determine the depth to magnetic sources in the area. Aeromagnetic signatures of the study area showed variations in high and low anomalies trending in the NE – SW, NW – SE, N – S and E – W directions. These anomalies aligned with the trends of the interpreted lineaments from the filtered maps. The AS and HGM maps delineated the edges of rounded, sub-rounded and elliptical source bodies interpreted to represent porphyritic ring dyke complexes that intruded the Precambrian Basement rocks underlining the study area. Estimated depths for shallow and deeper magnetic sources was 0.28 km and 2.86 km, respectively. Lineaments mapped in this study may have acted as conduits for the flow of hot mineralized hydrothermal fluids, and may therefore represent potential target zones for ore mineral exploration.

**Keywords:** *Structural analysis; Aeromagnetic data; Naraguta area; Hydrothermal mineralization.*

---

## 1. Introduction

The study area (Fig. 1) is located within the northcentral part of Nigeria on longitude 8°30' E - 9°00' E and latitude 9°30' N - 10°00' N, with an aerial coverage of about 3025 km<sup>2</sup>. The area is characterized by rugged topography defined by high relief features with elevation ranging from 550 m to more than 1300 m. The area has attracted interests from the solid mineral sector, following the increase in demand for lithium, cassiterite, columbite and other critical elements needed in the production of batteries for electric vehicles (EVs). These minerals which are hosted in basement complex rocks like those of northcentral Nigeria, have been illegally exploited by local miners and artisans over the years [1-6].

Several researchers have carried out studies in attempt to characterize the structural disposition of the Naraguta area and environs, using various geological and geophysical techniques. [7] analyzed the structural trend and spectral depth of the area using residual magnetic field data. They observed several magnetic closures of different sizes trending in the NE – SW direction, which may be linked with the occurrence of younger granite rings in the study area. [8] carried out magnetic basement depth re-evaluation of the Naraguta and environs north-central Nigeria using 3D Euler deconvolution. They concluded that the area has potentials for solid mineral exploration due to the presence of several lineaments controlling ore deposits. [9] conducted mapping and analysis of the density of lineaments of the Younger Granite complexes of Jos and environs, northcentral Nigeria. They showed that the main structural trends of the lineaments are in the NE – SW, NW – SE, N – S, and E – W directions.

---

In this study, detailed structural analysis of high-resolution aeromagnetic data over the Naraguta area and environs, northcentral Nigeria was carried out to map lineaments and identify areas with high potentials for hydrothermal mineral exploration.

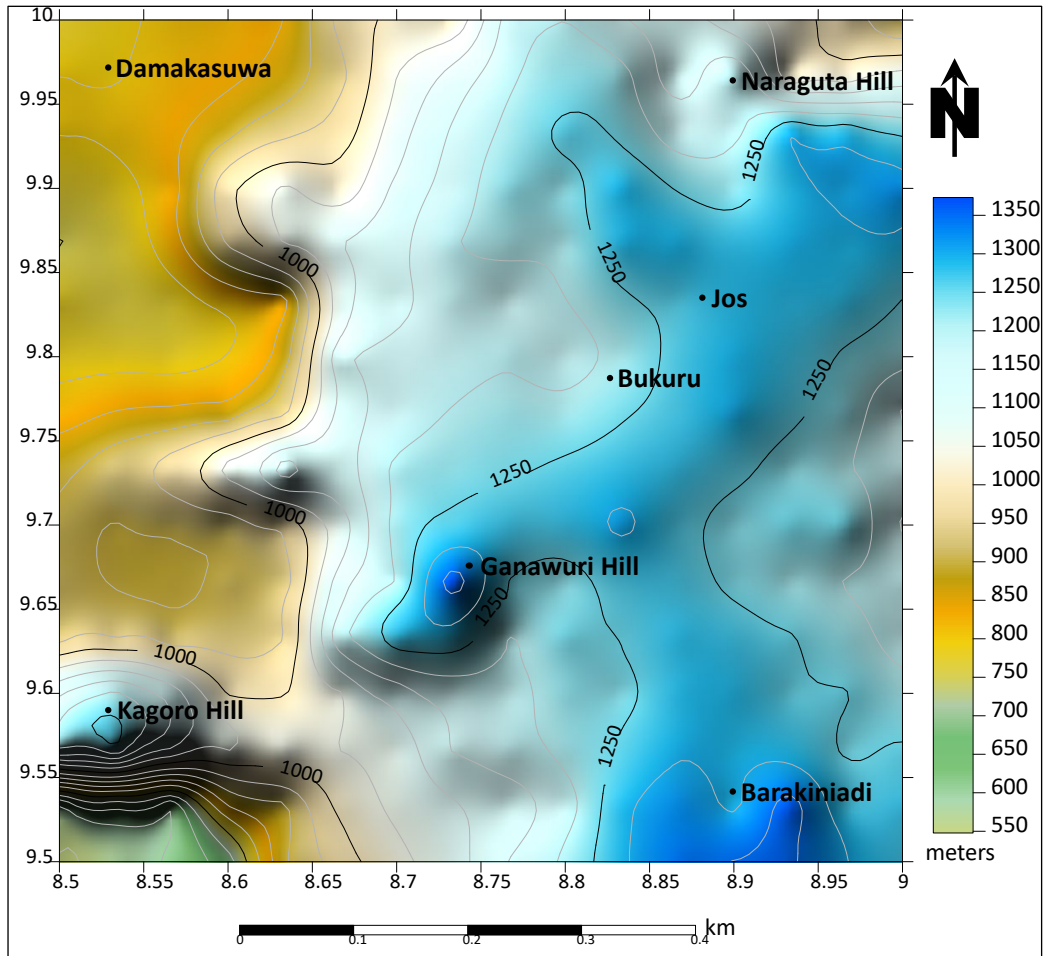


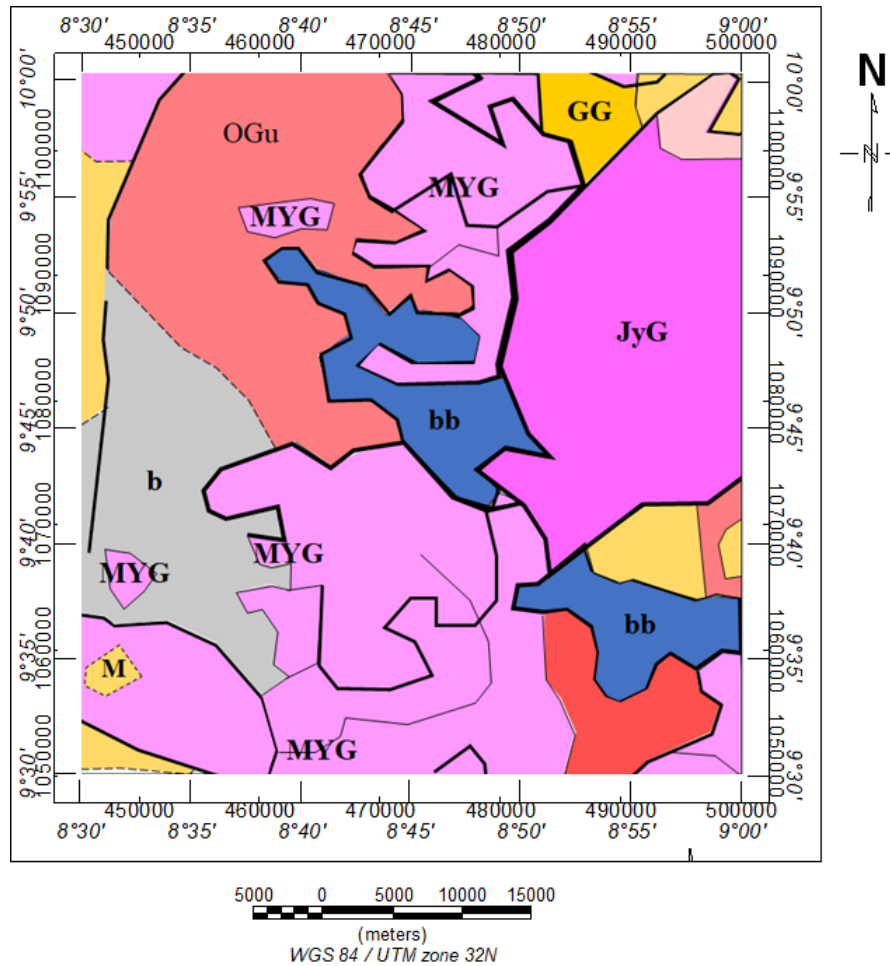
Fig. 1. Topographic map of the study area.

## 2. Geology of the area

The Naraguta and environs is underlain mostly by the Basement Complex rocks of north-central Nigeria, including the Migmatite-Gneiss Complex, the Younger Granite and the Basalts (Fig. 2.). The Migmatite-Gneiss complex occupies the northern part of the study area; the Younger Granites Ring Complexes are mostly found at the northeastern and southeastern parts, while the Basalts dominates the southwestern and central portions of the study area.

The Migmatite-Gneiss Complexes have been subjected to multiple episodes of deformation, including the Eburnean Orogeny ( $2000 \pm 200$  Ma), Kibaran ( $1100 \pm 150$  Ma) and Pan-African ( $600 \pm 150$  Ma) orogeny. These tectonic episodes resulted in the emplacement of the Older Granites [8,10].

Petrologically, the Younger Granites constitute mostly of distinctive crystalline granitic igneous rocks. Different Younger Granite Complexes of varying sizes have been mapped and given type names after their type localities. Each of the Younger Granite Rings maintain its distinct topographic characteristic, and form a range of plateau with elevation between 300 - 1100 m above the surrounding basement rocks. The rocks are composed mainly of four distinct lithologies, including Hornblende-Pyroxene-Fayalite granite, Hornblende-Biotite granite, Biotite granite and Riebeckite granite [11].



**Legend**

<b>b</b> Younger Basalt	<b>OGu</b> Undifferentiated granite, migmatite and granite Gneiss
<b>bb</b> Basalt	<b>GG</b> Granite Gneiss
<b>MYG</b> Granite and granite porphyry	<b>M</b> Migmatite
<b>JyG</b> Biotite granite	

Fig. 2. Geological map of the study area (after NGSA, 2004).

### 3. Materials and method

#### 3.1 Aeromagnetic data

The Naraguta area and environs is covered by aeromagnetic data sheet 168. Th data was obtained from the Nigerian Geological Survey Agency (NGSA) for this study. Acquisition of the data was carried out by Fugro for NGSA as part of the nationwide airborne surveys conducted between 2004 and 2009. The data was processed using software tools including Oasis Montaj, Surfer, MS Excel, and Matlab.

The total magnetic intensity (TMI) grid (Fig. 3) was reduced to the magnetic equator (RTE) to ensure that the anomalies are symmetrically centered over their causative sources. The RTE grid formed the basis for the application of different filtering techniques to delineate the contacts of linear geological features that may control hydrothermal mineralization in the study area.

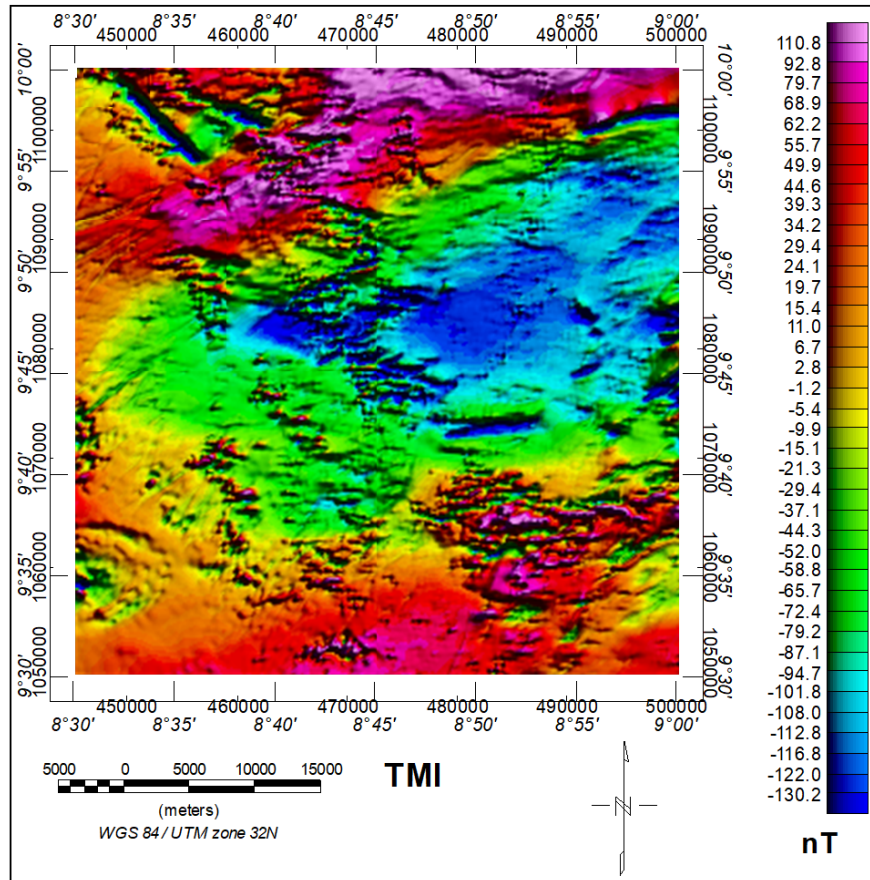


Fig. 3. Total magnetic intensity (TMI) map of the study area.

### 3.2. Data processing technique

Filtering techniques applied to the RTE data to enhance the edges of subsurface linear features in the study area include the first vertical derivative (1VD), analytical signal (AS) and horizontal gradient magnitude (HGM) [12-15]. Lineaments mapped from the filtered aeromagnetic grids were analyzed to obtain their structural trends using rose diagram plot. Determination of depth to the magnetic basement was achieved using the spectral analysis method. The routines adopted in this study are briefly described in the next paragraphs.

#### First vertical derivative (1VD)

The first vertical derivative filter estimates the vertical rate of change in the magnetic anomalies. It is a good filter for detecting shallow-seated geological features that exhibit short-wavelength anomalies [16]. It is mathematically given by the equation:

$$1VD = -\frac{\partial F}{\partial Z} \quad (1)$$

#### Analytical signal (AS)

This filter performs well at low latitudes, where it easily detects the contacts of steep dipping features at shallow depths [15,17]. It is given by the expression [12]:

$$|A(x, y)| = \sqrt{\left[\left(\frac{\partial T}{\partial x}\right)^2 + \left(\frac{\partial T}{\partial y}\right)^2 + \left(\frac{\partial T}{\partial z}\right)^2\right]} \quad (2)$$

where  $|A(x, y)|$  is the amplitude of the analytical signal at  $(x, y)$ ,  $T$  is the observed magnetic field at  $(x, y)$  and  $dT/dx$ ,  $dT/dy$  and  $dT/dz$  are the first derivative of the total magnetic field.

*Horizontal gradient magnitude (HGM)*

This is a common edge detection filter for identifying shallow linear structures like faults and fractures. It is defined as [18]:

$$HGM = \sqrt{\left(\frac{\partial M}{\partial x}\right)^2 + \left(\frac{\partial M}{\partial y}\right)^2} \quad (3)$$

where  $(\partial M/\partial x)$  and  $(\partial M/\partial y)$  are the horizontal derivatives of the magnetic field.

*Spectral analysis (SA)*

The basic principle of the spectral analysis method is by considering the integral of a magnetic field measurement at the surface from all depths. This can be performed by using the Discrete Fourier Transform - a mathematical tool for spectral analysis of aeromagnetic data. [19] proposed the use of the power spectrum method to analyze potential field data, while [20] deployed the technique to determine the depth to anomalous source bodies in the subsurface. The power spectrum derived from Fourier Transform of the magnetic field data can be used to estimate the average depths to magnetic source ensembles. The complex form of the two-dimensional Fourier transform pair is given by [19]:

$$G(u, v) = \iint_{-\infty}^{\infty} g(x, y) e^{i(u_x - v_y)} d_x d_y \quad (4)$$

$$G(x, y) = \frac{1}{4\pi^2} \int_{-\infty}^{\infty} g(u, v) e^{i(u_x - v_y)} d_x d_y \quad (5)$$

where  $u$  and  $v$  are the angular frequencies in  $x$  and  $y$  directions respectively.

$G(u, v)$  can be separated into its real and imaginary parts by using the expression:

$$G(u, v) = P(u, v) + iQ(u, v) \quad (6)$$

Then, the energy spectrum is given by the equation,

$$E(u, v) = [G(u, v)]^2 = (P^2 + Q^2) \quad (7)$$

[20] showed the energy spectrum can be expressed in polar form as follows:

if  $r^2 = (u^2 + v^2)$  and  $\theta = \text{arc tan}\left(\frac{u}{v}\right)$ , the energy spectrum  $E(r, \theta)$  could be given by:

$$\langle E(r, \theta) \rangle = 4\pi^2 M^2 R_G^2 (e^{-2hr}) ((1 - e^{-tr})^2) (S^2(r, \theta)) (R_p^2(\theta)) \quad (8)$$

where,  $\langle E(r, \theta) \rangle$  indicates the expected value;  $r^2 = (u^2 + v^2)$  is the magnitude of the frequency vector and  $\theta = \text{arc tan}\left(\frac{u}{v}\right)$  is the direction of the frequency vector.  $M$  is magnitude of the moment/unit depth;  $h$  is the depth to top of the prism;  $t$  is the thickness to top of the prism;  $S$  is the factor for the horizontal size of the prism;  $R_p$  is the factor for the magnetization of the prism and  $R_G$  is the factor for geomagnetic field direction.

The average depth  $h$  to the ensemble, enters only into the factor:

$$\{e^{-2hr}\} = \frac{e^{2hr} \sinh(2r\Delta h)}{4r\Delta t} \quad (9)$$

The energy spectrum will then consist of two parts; the low frequency part related to the deeper magnetic source and which decays rapidly, and the high frequency part which is associated with shallower magnetic sources dominance. Straight line slopes are often fitted to the radial spectrum to approximate the depths of the possible layers [20]. As shown by [21], the average depth to magnetic sources can be calculated as follows:

$$h(f) = \frac{M}{4\pi} M \times 0.08 \text{ cycles/unit distance} \quad (10)$$

$$h(f) = \frac{M}{2} M \times 0.5 \text{ radians/unit distance} \quad (11)$$

where,  $M = \frac{\text{Log } E}{f}$  is the gradient and  $E(f) = e^{-2hf}$  is the energy spectrum and  $\text{Log } E$  is the variation of the logarithm of the power spectrum in the interval of frequency.

The procedure described above for spectral analysis was adopted in this study to determine the depths to magnetic sources. The RTE data was sub-divided into 25 blocks (Fig. 4), and each of the blocks were analyzed to obtain the radial average power spectrum (Fig. 5) using the Fast Fourier Transform (FFT) technique. Straight-line slopes were fitted to obtained 2D power curves to estimate the depths to magnetic source bodies in the study area.

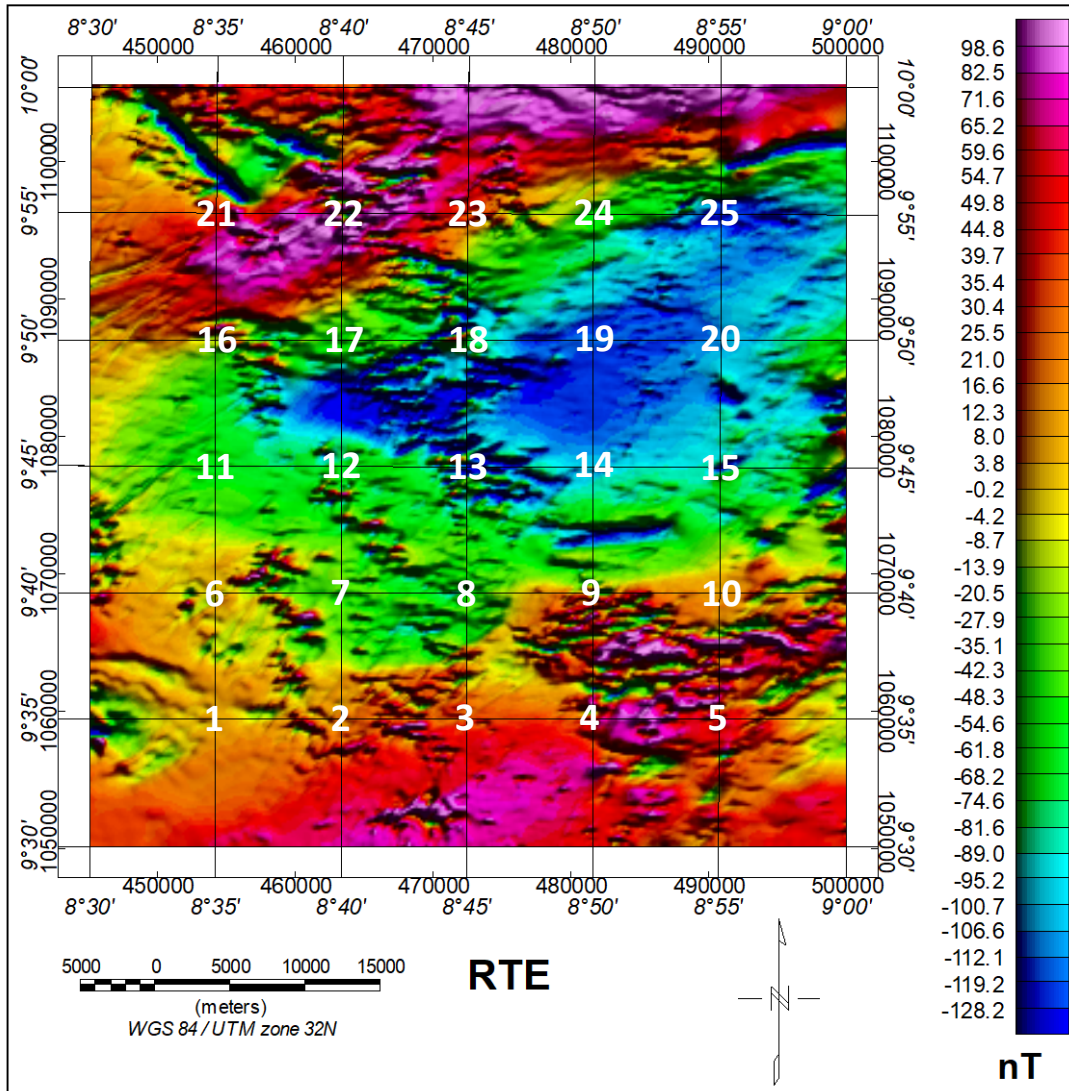


Fig. 4. RTE map of the study area showing the spectral blocks.

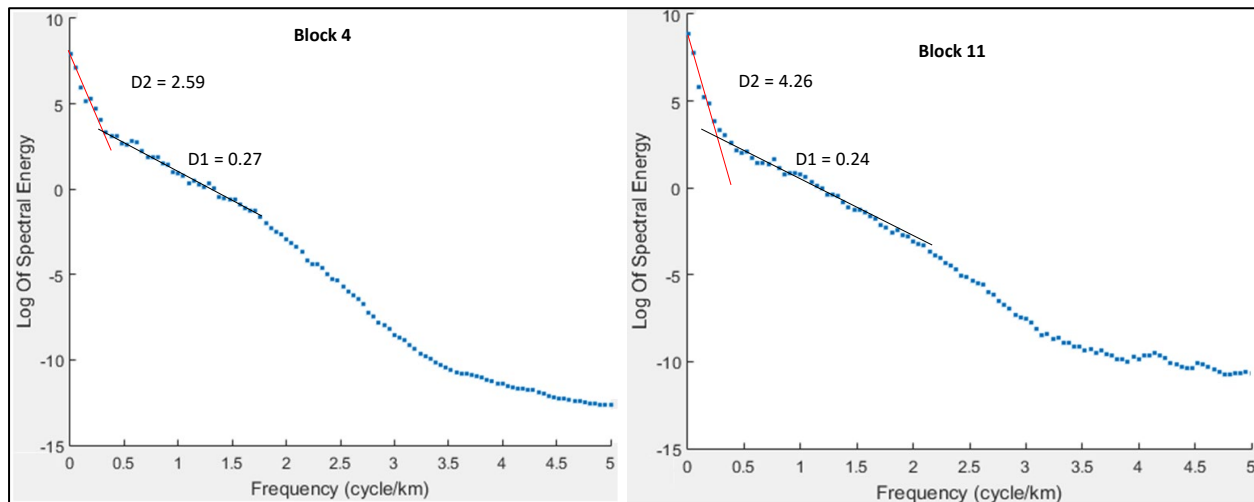


Fig. 5. Radial averaged power spectrum of Blocks 4 and 11.

## 4. Results and discussion

### 4.1. RTE map of the study area

The reduced to the equator magnetic intensity map (Fig. 4) of the study area showed alternations in high, low and intermediate magnetic anomalies representing the varying nature in magnetic susceptibility of the subsurface rocks. The anomaly variations trend mostly in the NE-SW, NW-SE, N - S and E - W directions respectively. High anomaly values ranging between -4.2 – 98.6 nT dominate the northern and southern portions of the RTE map, while the central part of the map is dominated by intermediate to low anomalies between -128.2 and -8.7 nT. The observed magnetic signatures in the study area are characterized by sharp magnetic boundaries, emanating from vertical or high-angle dipping faults and fractures. The aeromagnetic signatures follow the trend of subsurface geological features responsible for the observed anomalies.

### 4.2. Lineaments interpretation and structural trend

Subsurface linear geological features that may control mineralization were delineated on the 1VD and HGM maps of the study area obtained by applying edge enhancement filtering to the aeromagnetic data. The first vertical derivative map (Fig. 6) showed anomaly values ranging between -0.214 – 0.198 nT. The map revealed cluster of lineaments at the central part of the study area. These linear features trend in the NW – SE direction, with their conjugate NE – SW oriented features. Other highlighted structural contacts trend in the N – S and E – W directions. The features described above were highlighted by the HGM map (Fig. 7), which also delineated the trend of intrusive rocks in the study area. The map showed magnetic anomalies ranging from 0.003 to 0.286 nT.

The identified lineaments in the study area show major trends in the NE – SW, NW – SE, N – S and E - W directions, as observed from the rose diagram plot (Fig. 8). These trends conform with major structural orientations in the Nigeria Basement Complex terrain and the Benue Trough [8,22-23].

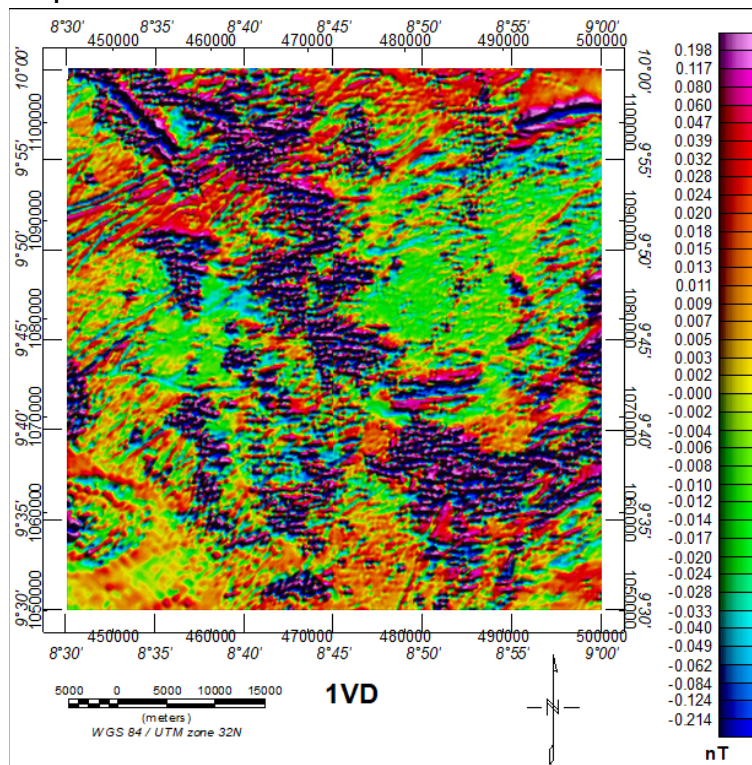


Fig. 6. 1VD map of the study area.

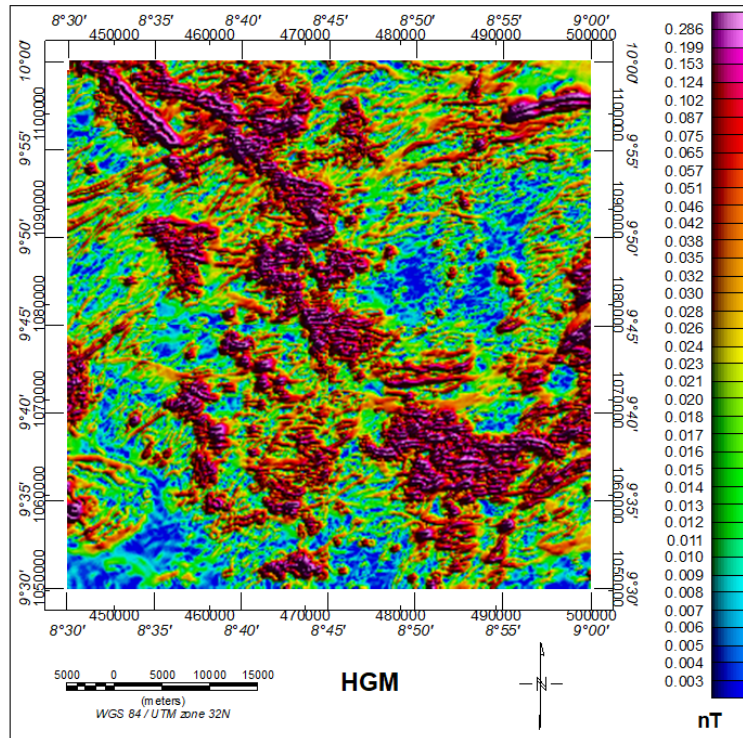


Fig. 7. HGM map of the study area

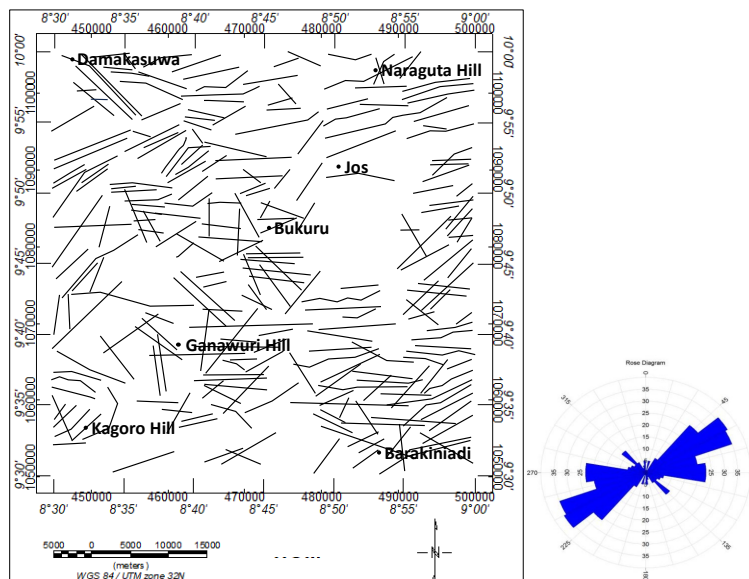


Fig. 8. Lineament map of the study area, with rose diagram showing the main structural trends.

[24] and [25] have shown that the Nigerian Basement Complex is characterized by NE - SW trending lineaments that could be correlated to the Romanche and Chain Fracture Zones in the Gulf of Guinea. The NE - SW trends, with their conjugate NW - SE lineaments represents younger tectonic episodes that affected the basement, and obliterated the older, deeper E - W and N - S tectonic trends, which were reactivated from crustal zones of weakness in the basement as a result of the late Phanerozoic plate tectonic event [26].

Magnetic depth to basement maps of the study area revealed that the lineaments occur at depths closer to the surface (Fig. 9 and Fig. 10), with an average depth of 0.28 km to shallow basement sources (D1) and an average depth of 2.86 km to deeper sources (D2) (Table 1).

Table 1. Estimated depths to shallow (D1) and deeper (D2) magnetic sources in the study area.

Block	X	Y	D1 (km)	D2 (km)
1	454143	1059514	0.31	3.34
2	463428	1059454	0.24	2.67
3	472469	1059399	0.22	2.51
4	481709	1059399	0.27	2.59
5	490795	1059508	0.35	1.64
6	454234	1068648	0.32	1.71
7	463483	1068703	0.33	3.42
8	472263	1068648	0.22	3.12
9	481763	1068648	0.28	1.26
10	490958	1068648	0.34	1.95
11	454288	1077788	0.24	4.26
12	463374	1077788	0.27	3.6
13	472263	1077897	0.24	3.06
14	481763	1077897	0.37	3.43
15	490903	1077843	0.38	4.03
16	454342	1087038	0.24	2.75
17	463483	1087038	0.24	2.94
18	472569	1087038	0.22	2.99
19	481709	1087092	0.23	2.77
20	490849	1087038	0.28	4.3
21	454342	1096287	0.31	2.69
22	463483	1096341	0.27	2.77
23	472569	1096341	0.27	2.04
24	481654	1096287	0.18	2.22
25	490903	1096287	0.41	3.37
Average			0.28	2.86

Areas with high concentration of longer lineament lengths possess high potentials for hydrothermal mineralization. These areas were mostly observed to coincide with zones where the Younger Granite Ring complexes occurred in the study area [27]. The lineaments may have acted as flow pathways for hot hydrothermal fluids from the deeper parts of the earth [28-29].

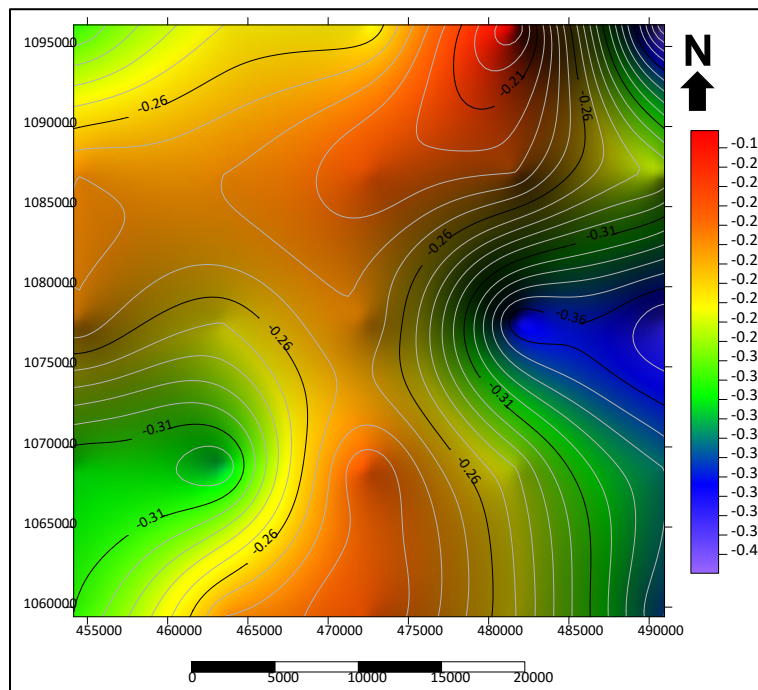


Fig. 9. Depth to shallow magnetic basement sources (D1).

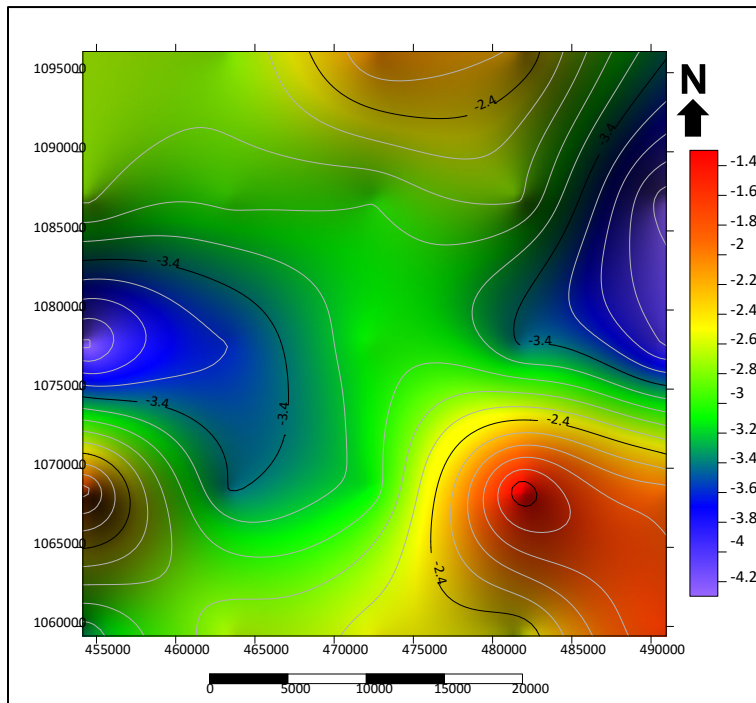


Fig. 10. Depth to deeper magnetic basement sources (D2).

#### 4.3. Identification of potential mineralization zones in the study area

The analytical signal (AS) map (Fig. 11) revealed high amplitude anomalies ranging between 0.036 – 0.429 nT in the central part of the study area.

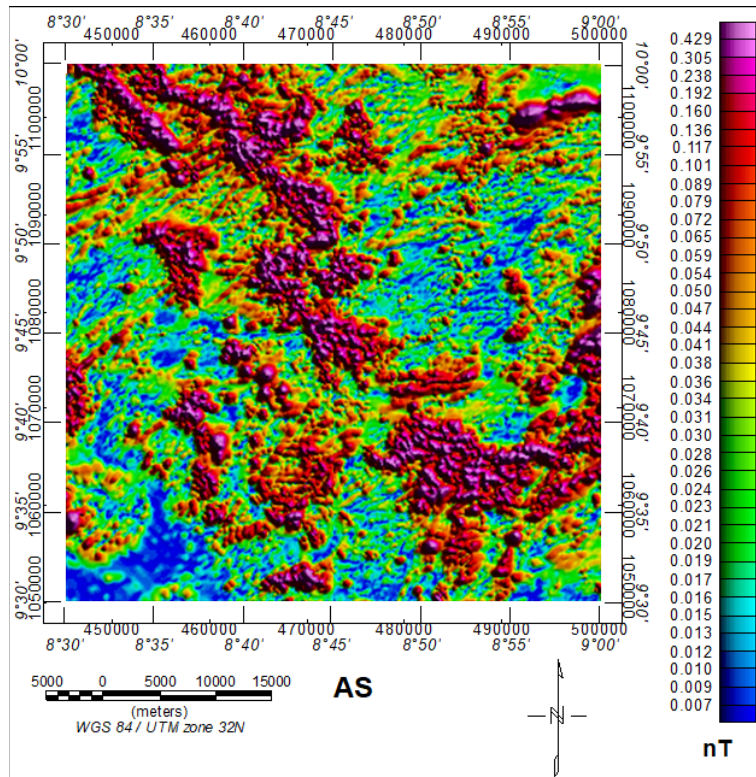


Fig. 11. Analytical signal map of the study area.

The trend of these anomalies was observed to coincide with the lineament directions. The AS filter clearly delineated the edges of rounded, sub-rounded and elliptical source bodies that represents dykes and porphyritic ring dyke complexes that intruded the basement rocks. These appeared as clusters of high amplitude peaks that were distributed in the central portion of the study area. The structures reflect the various tectono-deformational events that have impacted the basement, leading to different metamorphic grades and variations in magnetic susceptibilities of the underlying rocks.

High AS amplitude anomalies have been linked mineralized pegmatite fields in the parts of the Precambrian Basement Complex of southwestern Nigeria [6]. The high amplitude zones identified on the AS map represents potential mineralization zones in the study area. These areas are known to be associated with the occurrence of ore deposits like cassiterite, tin and columbite [27]. The interconnected longer lineaments lengths may have served as conduits for the flow of hot hydrothermal solutions and therefore control mineralization in these areas.

The structural framework of the study area reflects polycyclic and polyphase deformational episodes that promoted the enrichment of hydrothermal minerals. For instance, the lineaments around the Kagoro Hill, Ganawuri Hill, and Barakiniadi area, have high density and cuts across each other (Fig. 8). Areas with high lineament density have great potentials for hydrothermal mineralization and groundwater prospecting [28-29]. The lineaments were observed to occur mostly in area where the Younger Granites intruded and were uplifted closer to the surface, suggesting that they are products of past tectono-stress episodes and magmatic activities that affected the basement rocks in the area [11].

## 5. Conclusions

Structural analysis of high-resolution aeromagnetic data over the Naraguta area northcentral Nigeria, have been attempted in this study. The reduced to the equator (RTE) aeromagnetic data showed alternations in high and low magnetic signatures, reflecting variations in the magnetic susceptibility of the subsurface rocks. Structural enhancement filters applied to the RTE grid highlighted the edges of lineaments trending in the NE – SW, NW – SE, N – S and E – W directions. Spectral depth estimations revealed that these causative magnetic sources occur at shallow depths. Analytical signal filtering detected high amplitude peaks distributed in the central portion of the study area. These anomalous zones follow the main structural trends in the study area and thus, indicate potential zones of hydrothermal mineralization. The rounded, sub-rounded and elliptical shapes of the source bodies suggested that the anomalies emanated from porphyritic ring dyke complexes that intruded the Precambrian Basement rocks. The lineaments and dykes mapped in the study area may have served as pathways for the flow of hot mineralized hydrothermal fluids, and therefore represent potential targets for ore mineral exploration.

## References

- [1] Okunlola OA. Metallogeny of Ta-Nb Mineralization of Precambrian Pegmatite of Nigeria. *Mineral Wealth*, 2005; 38 - 50.
- [2] Okunlola OA, Oyedokun MO. Compositional trends and rare metal (Ta-Nb) mineralisation potential of pegmatite and associated lithologies of Igbetti area, southwestern Nigeria. *RMZ Mater. Geoenviron*, 2009; 56 (1): 38–53.
- [3] Adetunji A., Ocan OO. Characterization and mineralization potentials of granitic pegmatites of Komu area, southwestern Nigeria. *Resour. Geol.*, 2010; 60: 87 - 97.
- [4] Akinola OO, Okunlola OA, Obasi RA. Physico-chemical characteristics and industrial potentials of lepidolite from Ijero-Aramoko pegmatite field, southwestern Nigeria. *Int. J. Sci. Technol. Res.*, 2014; 3 (3): 278 - 284.
- [5] Obasi RA, Talabi AO, Madukwe H. Rare earth element geochemistry of stream sediments from pegmatite terrain of Ijero-Ekiti, southwestern Nigeria: implications for source rocks and paleo-oxidation conditions. *Int. J. Basic Appl. Sci. IJBAS IJENS*, 2018; 18 (2): 8 - 18.
- [6] Amigun JO, Sanusi SO, Audu L. Geophysical characterization of rare earth element and gemstone mineralization in the Ijero-Aramoko pegmatite field, southwestern Nigeria. *J. Afr. Ear. Sci.*, 2022; 188: 1 - 19.

- [7] Akanbi ES, Mangset WE. Structural trends and spectral depth analysis of the residual magnetic field of Naraguta area, North central, Nigeria. *Indian J. Sci. Technol.*, 2011; 4 (11): 1410 – 1415.
- [8] Opara AI, Emberga TT, Oparaku OI, Essien AG, Onyewuchi RA, Echetama HN, Muze NE, Onwe RM. Magnetic basement depth re-evaluation of Naraguta and environs North Central Nigeria, Using 3-D Euler deconvolution. *Am J Min Metall.*, 2015; 3 (2): 29-42.
- [9] Bulus JA. Mapping and analysis of the density of lineaments of the Younger Granite Complexes of Jos and environs Northcentral Nigeria. *Sci. Wor. J.*, 2021; 16 (3): 272 – 279.
- [10] Bird D. Shear margins continent-ocean transform and fracture zone boundaries. *Lead Edge*, 2001; 20 (2): 150-159.
- [11] Obaje NG. *Geology and mineral resources of Nigeria*. Springer, Berlin, 2009. <https://doi.org/10.1007/978-3-540-92685-6>
- [12] Roest WR, Verhoefs J, Pilkington M. Magnetic interpretation using 3-D analytic signal Magnetic interpretation using the 3-D analytic signal. *Geophysics*, 1992; 57 (1): 116–131. <https://doi.org/10.1190/1.1443174>
- [13] Blakely RJ. *Potential theory in gravity and magnetic applications*. Cambridge 757 University Press, 1995; 81- 87. <https://doi.org/10.1017/CB09780511549816>
- [14] Verduzco B, Fairhead JD, Green CM, Mackenze C. New insights into magnetic derivatives for structural mapping. *Lead Edge*, 2004; 23 (2): 116–119. <https://doi.org/10.1190/1.1651454>
- [15] Nabighian MN, Grauch VJS, Hansen RO, LaFehr TR, Li Y, Peirce JW, Philips JD, Ruder ME. The historical development of the magnetic method in exploration. *Geophysics*, 2005; 33 – 61. <https://doi.org/10.1190/1.2133784>
- [16] Milligan PR, Gunn PJ. Enhancement and presentation of airborne geophysical data. *AGSO J. Aust. Geol. Geophys.*, 1997; 17(2): 63 - 75. <https://pid.geoscience.gov.au/dataset/ga/81493>
- [17] Li X. Understanding 3D analytic signal amplitude. *Geophysics*, 2006; 71 (2), 13 - 16. <https://doi.org/10.1190/1.2184367>
- [18] Cordell L, Grauch VJS. Mapping basement magnetization zones from aeromagnetic data in the San Juan Basin, New Mexico. In the *Utility of regional gravity and magnetic anomaly maps*; Hinze WJ Ed. Society of Exploration Geophysicists, 1985; 181–197.
- [19] Bhattacharyya BK. Continuous spectrum of the total magnetic field anomaly due to rectangular prismatic body. *Geophysics*, 1966; 31: 197 – 212. <http://dx.doi.org/10.1190/1.1439767>
- [20] Spector A, Grant FS. Statistical models for interpreting aeromagnetic data. *Geophysics*, 1970; 35 (2), 293–302. <https://doi.org/10.1190/1.1440092>
- [21] Hinze WJ, Von Frese RRB, Saad AH. *Gravity and magnetic exploration principles, practices, and applications*. Cambridge University Press, New York, 2013. <https://doi.org/10.1017/CBO9780511843129>
- [22] Nwokocha KC. Interpretation of aeromagnetic and landsat ETM plus data over part of the Younger Granite Complex, Nigeria: implication for geothermal exploration. Unpublished MSc Thesis, Federal University of Technology, Owerri, 2016: 1 - 120.
- [23] Choko C, Ehirim CN, and Ebeniro JO. Indications of Hydrocarbon Prospects in the Lower Benue Trough from Aeromagnetic Data. *Pet Coal*, 2023; 65 (2): 261-270.
- [24] Ajakaiye DE, Hall DH, Ashiekaa JA, Udensi EE. Magnetic anomalies in the Nigerian continental mass based on aeromagnetic surveys. *Tectonophysics*, 1991; 192: 211 - 230.
- [25] Megwara JU, Udensi EE. Structural Analysis Using Aeromagnetic Data: Case Study of Parts of Southern Bida Basin, Nigeria and the Surrounding Basement Rocks. *Earth Science Research*, 2014; 3 (2): 27 - 38.
- [26] Ojo SB. Origin of a major aeromagnetic anomaly in the Middle Niger Basin, Nigeria. *Tectonophysics*, 1990; 185 (1): 153 - 162.
- [27] Nigerian Geological Survey Agency (NGSA). *Geology and mineral resources of North Central Zone Nigeria, NGSA Regional geology and mineral series*, 2008; 1: 1 - 29.
- [28] Okeke CJ, Ukaegbu VU, Egesi N. Remote sensing signature of geological structures inferred on landsat imagery of Afikpo area Southeastern Nigeria. *J. Geol. and Min. Res.*, 2019; 11 (1): 1-13.
- [29] Alkali SC. Mapping and analysis of the density of lineaments around Kagoro Younger Granite rocks in northcentral Nigeria. *Global Advanced Research Journal of Engineering, Technology and Innovation*, 2013; 2 (10): 295 - 303.

To whom correspondence should be addressed: Dr. Eze M. Okoro, Department of Geology, University of Nigeria Nsukka, Enugu State, Nigeria, E-mail: [ezemartok@gmail.com](mailto:ezemartok@gmail.com)